



Ain Shams University  
Ain Shams Engineering Journal

[www.elsevier.com/locate/asej](http://www.elsevier.com/locate/asej)  
[www.sciencedirect.com](http://www.sciencedirect.com)



## ELECTRICAL ENGINEERING

# Modeling and design considerations of a photovoltaic energy source feeding a synchronous reluctance motor suitable for pumping systems

M. Nabil <sup>a,\*</sup>, S.M. Allam <sup>b</sup>, E.M. Rashad <sup>b</sup>, SMIEEE

<sup>a</sup> *Department of Electrical Engineering, Kafrelshiekh University, Egypt*

<sup>b</sup> *Department of Electrical Power and Machines Engineering, Tanta University, Egypt*

Received 3 December 2011; revised 26 April 2012; accepted 8 May 2012

Available online 13 June 2012

### KEYWORDS

Photovoltaic energy source;  
Synchronous reluctance motor;  
Design consideration;  
Modeling;  
Pumping system

**Abstract** This paper presents the performance analysis of a photovoltaic (PV) energy source driving a synchronous reluctance (SyncRel) motor. The design considerations of the PV array, suitable for driving a centrifugal pump, are studied. Three design approaches are proposed at an average insolation of 0.5 kW/m<sup>2</sup>. These approaches depend upon determining the system operating point firstly and then maintaining this point on the PV generator characteristics. The first approach takes motor starting current into account as an additional design criterion. The second one is based on achieving the maximum power at the system operating point. The third approach considers maintaining voltage regulation of the PV generator at a pre-specified suitable value. A sample of the simulation results is introduced using the SyncRel motor measured parameters and the estimated parameters of the PV array. It has been found that the minimum number of cells can be achieved using the second approach.

© 2012 Ain Shams University. Production and hosting by Elsevier B.V.  
All rights reserved.

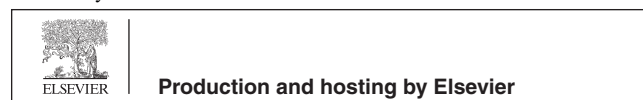
### Contents

1. Introduction . . . . .	376
2. System modeling . . . . .	376

\* Corresponding author. Tel.: +20 1095147805.

E-mail addresses: [m.nabil\\_it@yahoo.com](mailto:m.nabil_it@yahoo.com) (M. Nabil), [sm\\_allam@yahoo.com](mailto:sm_allam@yahoo.com) (S.M. Allam), [emrashad@ieee.com](mailto:emrashad@ieee.com) (E.M. Rashad).

Peer review under responsibility of Faculty of Engineering, Ain Shams University.



2.1.	PV generator model	377
2.2.	Inverter model	377
2.3.	Synchronous reluctance motor model	377
2.4.	Centrifugal pump model	377
3.	Design approaches	378
4.	Results and discussions	378
4.1.	The first approach	379
4.2.	The second approach	380
4.3.	The third approach	381
5.	Conclusions	381
	References	382

### Nomenclature

$B$	viscous friction coefficient, N m/rad/s	$P_o$	output power of the motor, W
$C$	proportionality factor of the pump, N m/rad/s	$Q$	flow rate, m <sup>3</sup> /h
$H$	total pumping head, m	$r_{dr}, r_{qr}$	direct and quadrature axis rotor resistance of SyncRel motor respectively, $\Omega$
$I_{ds}, I_{qs}$	direct and quadrature axis stator current respectively, A	$R_s$	stator resistance of SyncRel motor, $\Omega$
$I_g$	current drawn from the array, A	$T_e$	electromagnetic torque of the motor, N m
$J$	inertia of the system, kg m <sup>2</sup>	$T_o$	constant torque of the pump, N m
$L_{ds}, L_{qs}$	direct and quadrature axis stator inductance of SyncRel motor respectively, H	$V_{ds}, V_{qs}$	direct and quadrature component of stator voltage respectively, V
$L_{md}, L_{mq}$	direct and quadrature axis magnetization inductance respectively, H	$V_g$	terminal voltage of the array, V
$P$	number of pole pairs	$V_m, V$	maximum and effective values of the motor input voltage respectively, V
$p$	differential operator (d/dt)	$\delta$	load angle, rad
$P_g$	output power of the array, W	$\omega_r$	motor speed, rad/s
$P_{in}$	input power of the motor, W		

## 1. Introduction

Recently, the implementation of renewable energy resources, such as solar and wind, for electrical power applications has received a considerable attention. Since solar energy is free, inexhaustible and clean, it has a great potential to be a very attractive supply option for industrial and domestic applications such as water pumping, heating and cooling. Solar photovoltaic system uses the PV modules in order to convert the sunlight into electrical energy. PV generation is gaining increased importance as renewable source due to its advantages like little maintenance requirements, absence of fuel cost, no noise due to absence of moving parts [1]. In particular, the photovoltaic pumping systems are receiving more attention in recent years especially in remote areas where connection to the grid is technically not possible or costly [2].

The dc motor can be directly connected to the photovoltaic generator and an adjustable dc drive is easy to be achieved. However, this system suffers from increased motor cost and maintenance problems due to the presence of commutator and brushes. Therefore, brushless motors represent an attractive alternative due to its merits over dc motors. A synchronous reluctance motor fed by a photovoltaic generator represents a brushless scheme that should be analyzed under different operating conditions.

The implementation of the PV energy sources for water pumping and irrigation applications based on dc motor [3,4],

an induction motor [2,5] and permanent magnet (PM) synchronous motor [6] has been found a considerable interest from researchers.

However, the photovoltaic pumping system based on a synchronous reluctance motor has not gained any significant attention from researchers until to date.

The aim of this paper is to present a mathematical model by which the performance analysis of a photovoltaic pumping system, based on a synchronous reluctance (SyncRel) motor, can be predicted. In addition, the paper aims at investigating the design considerations of the photovoltaic (PV) array, suitable for driving a centrifugal pump at an average insolation of 0.5 kW/m<sup>2</sup>.

## 2. System modeling

Fig. 1 shows a block diagram of the proposed system which consists of the following parts:

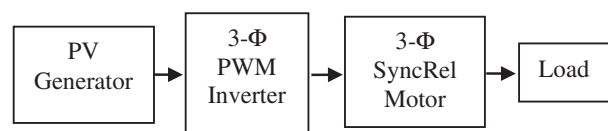
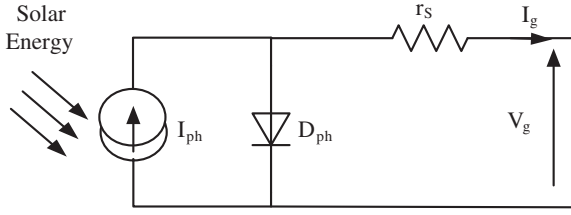


Figure 1 Block diagram of the proposed system.



**Figure 2** Equivalent circuit of a PV cell.

- Photovoltaic (PV) generator.
- Three-phase pulse width modulation (PWM) inverter.
- Three-phase synchronous reluctance (SyncRel) motor.
- Centrifugal pump load.

### 2.1. PV generator model

The PV generator converts the solar insolation into electric dc power. It consists of an array of PV cell modules connected in series–parallel combinations to provide the desired dc voltage and current. The terminal voltage, current and the internal resistance of the array depend on the number of series cells ( $N_s$ ), the number of parallel strings ( $N_p$ ) and the insolation of the region where the PV array is installed. The approximate equivalent circuit of a single cell is shown in Fig. 2 [7].

The terminal voltage of the PV array is given by [7]:

$$V_g = \left( \frac{T_c N_s k A}{q} \right) \ln \left( \frac{I_{ph} - I_g + N_p I_s}{N_p I_s} \right) - \left( \frac{N_p}{N_s} \right) I_g r_s \quad (1)$$

where  $T_c$  is the cell temperature,  $I_{ph}$  is the photocurrent,  $I_s$  is the saturation current,  $K$  is the Boltzmann constant ( $1.38 \times 10^{-23}$  J/K),  $A$  is the solar cell ideal factor of the diode,  $r_s$  is the series cell resistance and  $q$  is the electron charge ( $1.6 \times 10^{-19}$  C).

The photocurrent depends upon the solar insolation and the cell temperature. It can be described as [8]:

$$I_{ph} = (I_{sc} + k_i(T_c - T_{ref}))G \quad (2)$$

where  $I_{sc}$  is the cell short-circuit current at 25 °C and the standard value of a solar insolation ( $1 \text{ kW/m}^2$ ),  $k_i$  is the temperature coefficient of the cell short-circuit current ( $\text{A}/^\circ\text{C}$ ),  $T_{ref}$  is the cell reference temperature and  $G$  is a solar insolation ( $\text{kW/m}^2$ ).

The saturation current varies with the cell temperature as follows [8]:

$$I_s = I_{rs} \left( \frac{T_c}{T_{ref}} \right)^3 \exp \left( \frac{q E_G}{k A} \left( \frac{1}{T_{ref}} - \frac{1}{T_c} \right) \right) \quad (3)$$

where  $I_{rs}$  is the cell reverse saturation current at the reference temperature and the solar radiation and  $E_G$  is the bang-gap energy of the semiconductor used in the cell.

### 2.2. Inverter model

The inverter is used to convert the dc voltage to a three-phase voltage with variable amplitude and variable frequency.

A natural Pulse Width Modulation (PWM) switching technique is used to drive the inverter. The effective value of the fundamental motor phase voltage is given by [9]:

$$V = \frac{M V_g}{2\sqrt{2}} \quad (4)$$

where the modulation index  $M$  is the ratio between the reference sine wave and the triangular carrier wave. In the present work,  $M$  is assumed to be 0.85. In addition, the value  $\frac{M}{2\sqrt{2}}$  represents the inverter gain.

### 2.3. Synchronous reluctance motor model

In order to eliminate the time-varying inductances in the voltage equations, the machine was represented in the  $qd$ -axis reference frame. The  $q$ - $d$  axis reference frame is fixed in the rotor, which rotates at  $\omega_r$  [10].

The  $qd$ -axis voltage equations can be written as:

$$V_{qs} = R_s i_{qs} + p \lambda_{qs} + \omega_r P \lambda_{ds} \quad (5)$$

$$V_{ds} = R_s i_{ds} + p \lambda_{ds} - \omega_r P \lambda_{qs} \quad (6)$$

$$V_{qr} = r_{qr} i_{qr} + p \lambda_{qr} \quad (7)$$

$$V_{dr} = r_{dr} i_{dr} + p \lambda_{dr} \quad (8)$$

The  $qd$ -axis flux linkage relations are expressed as:

$$\lambda_{qs} = L_{qs} i_{qs} + L_{mq} i_{qr} \quad (9)$$

$$\lambda_{ds} = L_{ds} i_{ds} + L_{md} i_{dr} \quad (10)$$

$$\lambda_{qr} = L_{qr} i_{qr} + L_{mq} i_{qs} \quad (11)$$

$$\lambda_{dr} = L_{dr} i_{dr} + L_{md} i_{ds} \quad (12)$$

The electromagnetic developed torque can be obtained from the relation:

$$T_e = \frac{3}{2} P (\lambda_{ds} i_{qs} - \lambda_{qs} i_{ds}) \quad (13)$$

The electromechanical equation is given by:

$$T_e = J p \omega_r + B \omega_r + T_L \quad (14)$$

The machine power angle  $\delta$  can be calculated as:

$$\delta = \int (\omega_r - \omega_s) dt \quad (15)$$

The steady state  $qd$ -axis stator currents can be given by:

$$I_{qs} = \left( \frac{V}{D} \right) [X_{ds} \sin(\delta) + R_s \cos(\delta)] \quad (16)$$

$$I_{ds} = \left( \frac{V}{D} \right) [X_{qs} \cos(\delta) - R_s \sin(\delta)] \quad (17)$$

where  $D = X_{ds} X_{qs} + R_s^2$ .

The  $qd$ -axis supply voltage can be expressed as a function of the machine power angle as:

$$V_{qs} = V_m \cos(\delta) \quad (18)$$

$$V_{ds} = -V_m \sin(\delta) \quad (19)$$

### 2.4. Centrifugal pump model

The hydraulic output power of the pump can be characterized by [5]:

$$P_p = 2.725QH \quad (20)$$

The relation between the hydraulic output power ( $P_p$ ) of the pump and the mechanical input power ( $P_m$ ) can be defined as the pump efficiency and is given by [11]:

$$\eta_p = \frac{P_p}{P_m} \quad (21)$$

On the other hand, the load torque of the centrifugal pump is given by [7]:

$$T_L = T_o + C\omega_r^{1.8} \quad (22)$$

where  $T_o$  and  $C$  are constants.

### 3. Design approaches

Three approaches are proposed in the design process for selecting the PV generator parameters at an average insolation of  $0.5 \text{ kW/m}^2$ . These approaches depend upon determination the steady state operating point of the system ( $V_g, I_g$ ) firstly and then maintaining this point on the photovoltaic generator characteristics. In each approach, another criterion should be taken into account in order to complete the design process and obtain the final PV generator characteristics.

In the first approach, the selection of the PV generator parameters is based on the motor starting current in addition to the system operating point. In this approach, taking the motor starting current into account in the design process ensures the motor capability for starting with the rated conditions. This results in increasing the required total number of PV cells.

On the other hand, in the second approach, the steady state operating point ( $V_g, I_g$ ) is assumed to be corresponding to the maximum output power of the PV generator which equals to the required motor input power irrespective of the motor capability for starting with the rated conditions. Therefore, the required total number of PV cells in this approach is expected to be smaller than that obtained in the first approach.

In the third approach, the PV open circuit voltage is taken into consideration in the design process in order to guarantee the level of this voltage in a permissible range. The selection of the PV generator parameters in this approach is based on assuming a voltage regulation of 20% at an average insolation of  $0.5 \text{ kW/m}^2$ .

### 4. Results and discussions

In order to confirm the validity of the proposed design approaches, a sample of simulation results is introduced. The presented samples of the simulation results are obtained using the measured parameters of a synchronous reluctance motor

**Table 1** Parameters of PV cell.

Open circuit voltage, $V_{oc}$	0.54 V
Short circuit current, $I_{sc}$	0.8 A
Series cell's resistance, $r_s$	0.05 $\Omega$
Solar cell's ideal factor, $A$	3.0191
Short circuit current temperature coefficient, $k_i$	$3e^{-3} \text{ A}/^\circ\text{C}$
Reverse diode saturation current, $I_{rs}$	$0.5e^{-3} \text{ A}$
Reference cell's temperature, $T_{ref}$	$25^\circ\text{C}$
Band gap energy, $E_G$	2

**Table 2** Parameters of syncret motor.

Rated power, $P_o$	470 W
Rated voltage, $V$	200 V
Rated current, $I$	2 A
Stator resistance, $R_s$	10 $\Omega$
$q$ -Stator inductance, $L_{qs}$	0.2228 H
$d$ -Axis stator inductance, $L_{ds}$	0.6366 H
$q$ -Axis rotor inductance, $L_{qr}$	0.0177 H
$d$ -Axis rotor inductance, $L_{dr}$	0.0745 H
$q$ -Axis rotor resistance, $r_{qr}$	19.29 $\Omega$
$d$ -Axis rotor resistance, $r_{dr}$	38.9 $\Omega$
$q$ -Axis magnetization inductance, $L_{mq}$	0.2043 H
$d$ -Axis magnetization inductance, $L_{md}$	0.5621 H
Viscous friction, $B$	0.000005 N m/rad/s
Pole pairs, $P$	2
Moment of inertia, $J$	0.0015 $\text{kg m}^2$

**Table 3** Parameters of centrifugal pump.

$T_o$	0.3 N m
$C$	0.0003

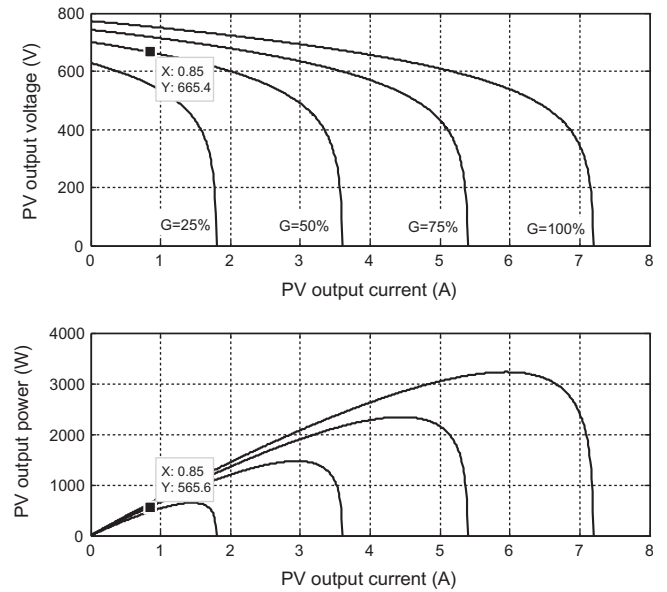


**Figure 3** Characteristics of the PV generator at different insolation level corresponding to the first approach.

rated at 470 W, 400 V and four-poles. The rotor is an axially laminated rotor type with cage to provide a starting torque. The parameters of the PV array are estimated depending upon the design approach. Appropriate parameters of the centrifugal pump parameters are selected.

All system parameters including PV cell, SyncRel motor and the centrifugal pump are given in Tables 1–4 respectively.

The PV generator operating point has been obtained for the following assumptions:

- The motor runs at its rated output power of 470 W
- The motor efficiency is 0.83 so that input motor power is 565 W.

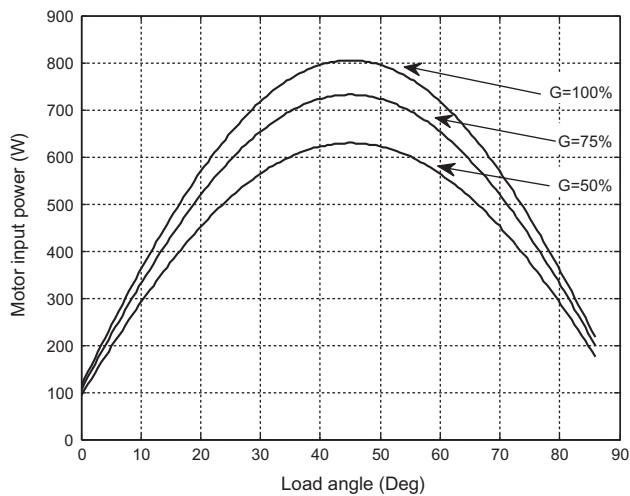


**Figure 4** Variation of the motor input power with the load angle corresponding to the first approach at different insolation level.

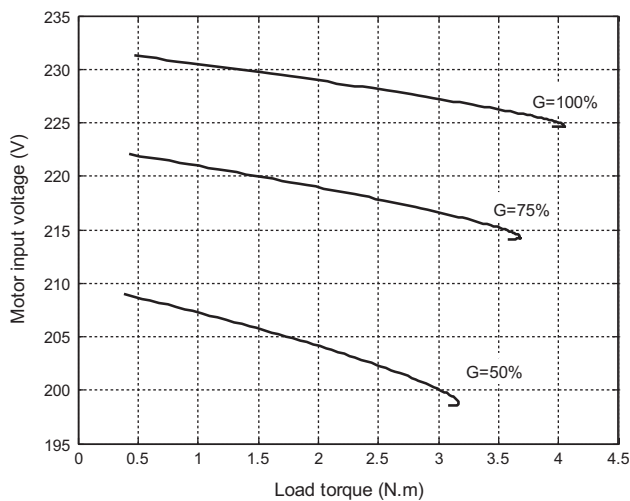


**Figure 5** Variation of the motor input voltage with the load torque corresponding to the first approach at different insolation level.

- The PV generator output equals the motor input power (assume lossless inverter)
- Considering the inverter gain, approximately equals 0.3 in the present work, the PV generator operating point is  $V_g = 665.5$  V and  $I_g = 0.85$  A.
- The motor is loaded by a suitable centrifugal pump which can be used in an irrigation system or other human needs. The used pump parameters are given in Table 3.

A sample of the obtained simulated results corresponding to the proposed three approaches can be presented as follows.

#### 4.1. The first approach

According to the first approach, considering the motor starting current and the daily average solar insolation level ( $G$ ) of

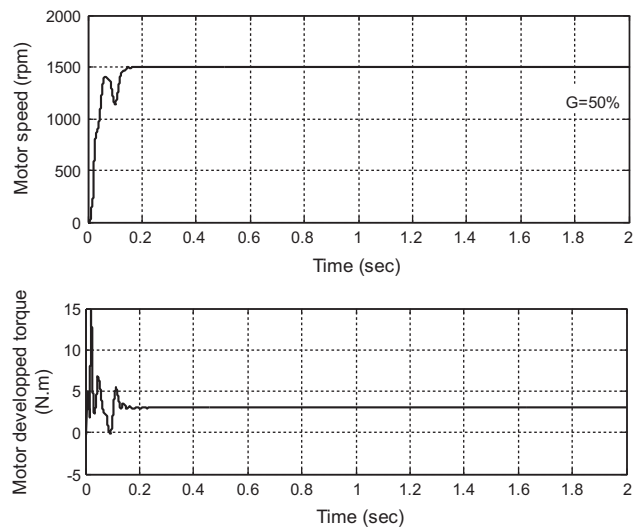


**Figure 6** Run-up response of a SyncRel motor under rated conditions corresponding to the first approach.

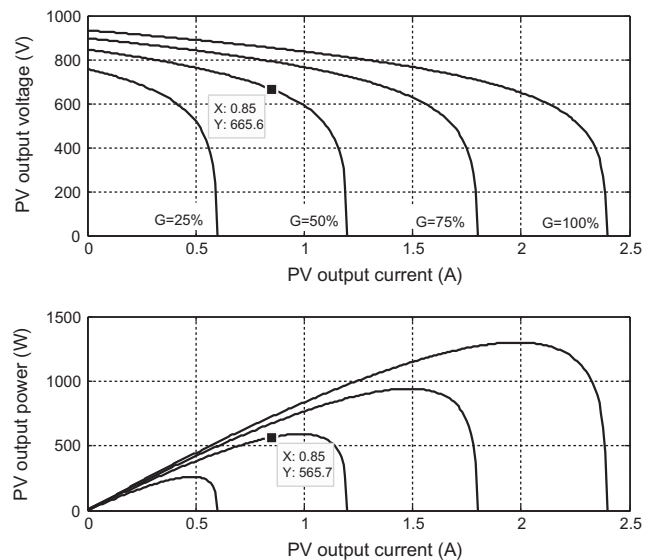
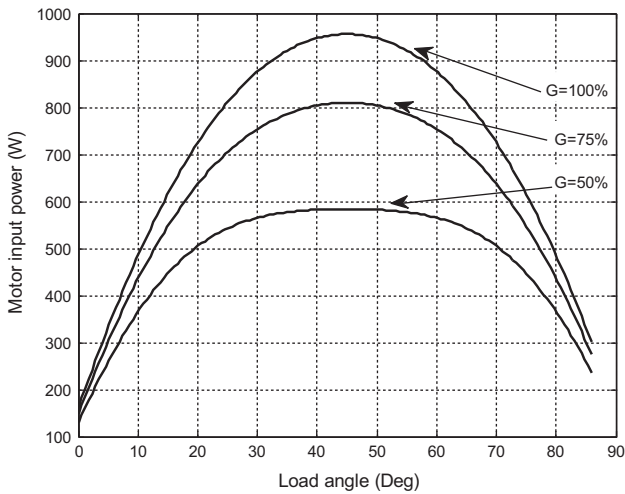


**Figure 7** Characteristics of the PV generator corresponding to the second approach at different insolation level.

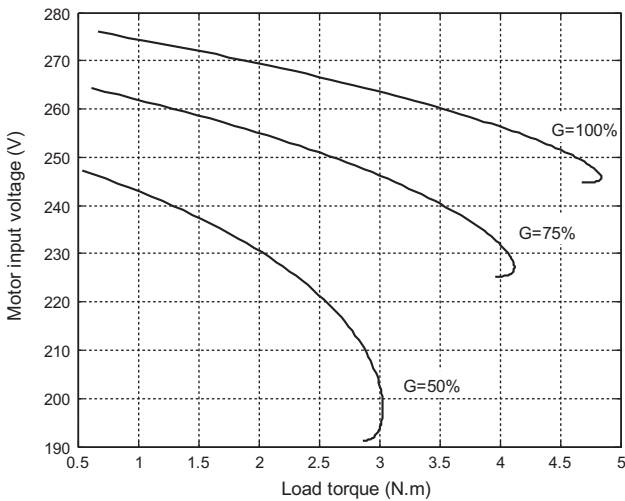
$0.5 \text{ kW/m}^2$ , the number of parallel strings ( $N_p$ ) and the number of series cells ( $N_s$ ) which gives this operating point ( $665.5$  V,  $0.85$  A) are 9 and 1433 respectively so that total number of cells are 12897.

Fig. 3 shows the characteristics of the PV generator at different solar insolation levels corresponding to the first approach. The variation of the motor input power with the load angle and the variation of the motor input voltage with load torque are shown in Figs 4 and 5 respectively. It can be observed that the motor is capable to operate with the rated load at insolation levels equal and higher than 50%.

Moreover, it can be observed from Fig. 5 that the no-load voltage is slightly higher than the rated value and the voltage regulation in this case is less than 20%.



**Figure 8** Variation of the motor input power with the load angle corresponding to the second approach at different insolation level.



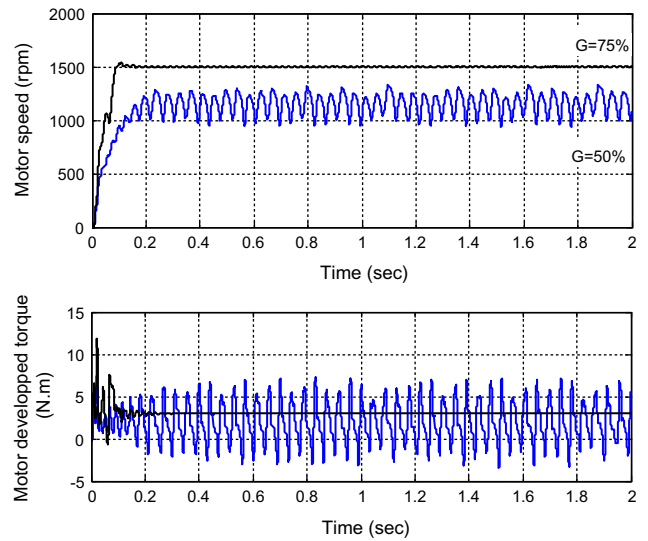
**Figure 9** Variation of the motor input voltage with the load torque corresponding to the second approach at different insolation level.

Fig. 6 shows the run-up response of the SyncRel motor under rated conditions corresponding to the first approach at an insolation level of 50%. It can be noted that the motor works stably with the rated conditions at this insolation level.

4.2. The second approach

With respect to the second approach, the number of parallel strings ( $N_p$ ) and the number of series cells ( $N_s$ ) which gives this operating point (665.5 V, 0.85 A) are 3 and 1730 respectively so that the total number of cells are 5190. In this case, this operating point corresponds to the maximum output power of the PV generator.

Fig. 7 shows the characteristics of the PV generator corresponding to the second approach at different solar insolation levels. The variation of the motor input power with the load angle and the variation of the motor input voltage with load



**Figure 10** Run-up response of a SyncRel motor under rated conditions corresponding to the second approach.

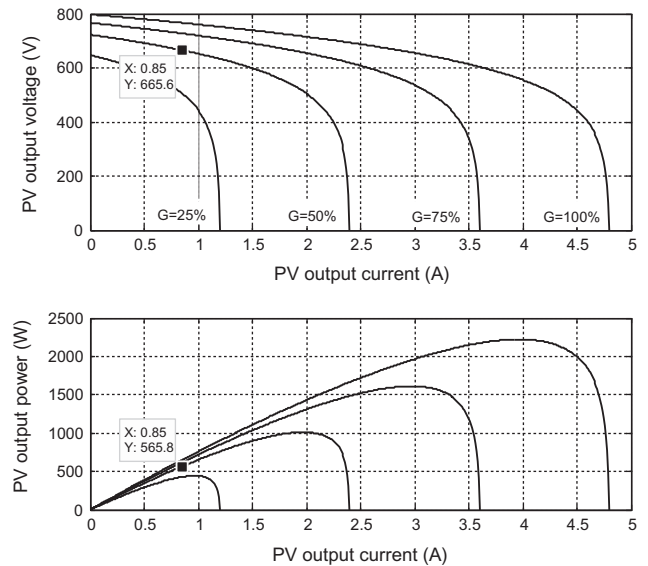


**Figure 11** Characteristics of the PV generator corresponding to the third approach at different insolation level.

torque are shown in Figs 8 and 9 respectively. The obtained results ensure that SyncRel motor operates stably at steady state with the rated load. However, it can be observed in this case that, there is no restriction on the no-load voltage and the voltage regulation in this case is higher than 20% as shown in Fig. 9. This is one of the problems exist in this approach and can be solved using any control scheme.

Fig. 10 shows the run-up response of the SyncRel motor under rated conditions corresponding to the second approach at insolation levels of 50% and 75%. It is clear that the motor is not stable with the rated conditions at an insolation level of 50%. At insolation levels equal or less than 50%, the starting problem may be solved using any control scheme However, this problem is solved at insolation levels higher than 50%.

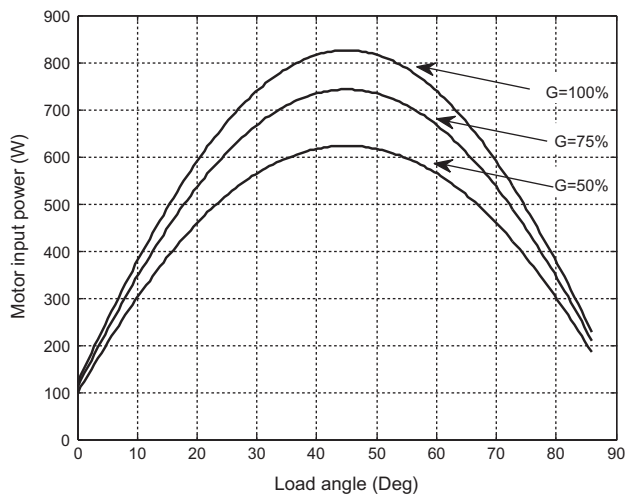


**Figure 12** Variation of the motor input power with the load angle corresponding to the third approach at different insolation level.

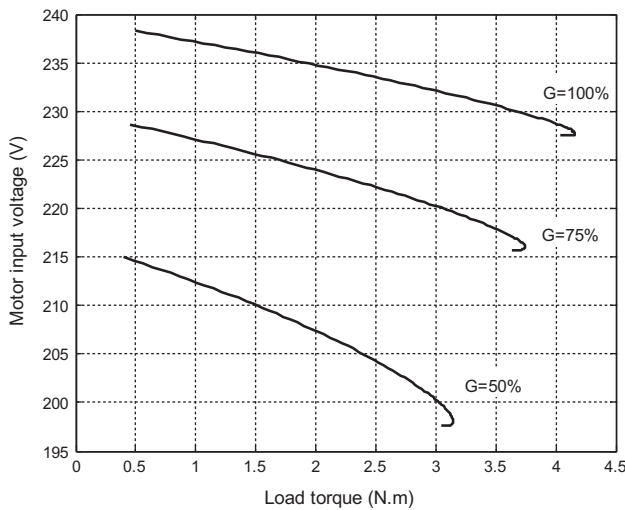


**Figure 13** Variation of the motor input voltage with the load torque corresponding to the third approach at different insolation level.

As shown in Fig. 10, the motor works stably with the rated conditions at an insolation level of 75%.

#### 4.3. The third approach

On the other hand, according to the third approach, considering the voltage regulation of 20% and the daily average solar insolation level ( $G$ ) of  $0.5 \text{ kW/m}^2$ , the number of parallel strings ( $N_p$ ) and the number of series cells ( $N_s$ ) which gives this operating point (665.5 V, 0.85 A) are 6 and 1480 respectively so that the total number of cells are 8880.

The characteristics of the PV generator, corresponding to the third approach, at different solar insolation levels is shown in Fig. 11. The variation of the motor input power with the load angle and the variation of the motor input voltage with load torque are shown in Figs. 12 and 13 respectively.

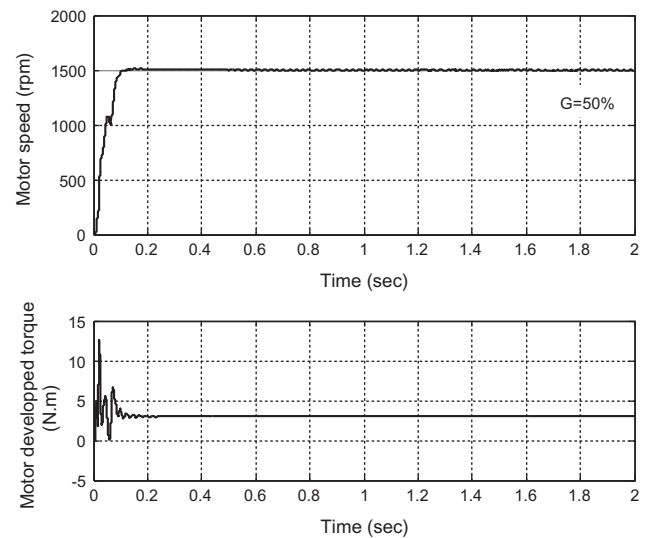


**Figure 14** Run-up response of a SyncRel motor under rated conditions corresponding to the third approach.

**Table 4** The final obtained results of the proposed three approaches.

Main features	Approach no.		
	1	2	3
Total number of cells	12897	5190	8880
Capability of starting with the rated conditions at $0.5 \text{ kW/m}^2$	Stable	Not stable	Stable
Voltage regulation	< 20%	> 20%	20%

Fig. 14 shows the run-up response of the SyncRel motor under rated conditions for  $N_p = 6$  and  $N_s = 1480$  at an insolation level of 50%. It is obvious that the starting problem is solved at this level of insolation.

## 5. Conclusions

This paper has presented a detailed modeling of a photovoltaic pumping system driven by a synchronous reluctance motor. The design considerations of the photovoltaic array, suitable for driving a centrifugal pump, have been investigated. Three approaches have been proposed in the design process, depending upon the operating point of the system. In these approaches, starting current, maximum power point or pre-specified voltage regulation has been taken into account. The final obtained results of the proposed three approaches can be concluded as shown in Table 4.

It has been found that using either the first or the third approach the motor works stably with the rated conditions at an average insolation level of  $0.5 \text{ kW/m}^2$ . However, the number of cells used in the first approach is higher than the third approach. Moreover, the voltage regulation equals or less than 20% using the third and the first approach respectively.

On the other hand, it has been observed that the minimum number of cells can be achieved using the second approach. However, the motor is not stable at an average insolation level of  $0.5 \text{ kW/m}^2$  and the voltage regulation is higher than 20%.

This problem is expected to be solved when controlling the inverter output by changing the modulation index.

## References

- [1] Betka Achour. Perspectives for the sake of photovoltaic pumping development in the south. Doctoral thesis; 2005.
- [2] Moussi A, Betka A. Performance optimization of a photovoltaic induction motor pumping system. *Renew Energy* 2004;29.
- [3] Chary Mummadi Veera. Steady-state and dynamic performance analysis of PV supplied dc motors fed from intermediate power converter. *Sol Energy Mater Sol Cell* 2000;61.
- [4] Rashad EEM, Shokralla SS. PV system fed DC motor controlled by boost converter. *Eng Res Bull* 1999;22(2).
- [5] Daud Abdel-Karim, Mahmoud Marwan M. Solar powered induction motor-driven water pump operating on a desert well. *Renew Energy* 2005;30.
- [6] Chenni R, Zarour L, Bouzid A, Kerbach T. Comparative study of photovoltaic pumping systems using a permanent magnet synchronous motor (PMSM) and an asynchronous motor (ASM). *Rev Energy Ren* 2006;9.
- [7] Alghuwainem SM. Steady-state performance of dc motors supplied from photovoltaic generators with step-up converter. *IEEE Trans Energy Convers* 1992;7(2).
- [8] Tsai Huan-Liang, Tu Ci-Siang, Su Yi-Jie. Development of generalized photovoltaic model using matlab/Simulink. In: *Proceedings of the world congress on engineering and computer science*, San Francisco, USA; 2008.
- [9] Mohan N, Undeland T, Robbins W. *Power electronics converters, applications and design handbook*, 2nd ed. New York: John Wiley & Sons, Inc; 1995.
- [10] Ferraz CAMD, deSouza CR. Reluctance synchronous motor asynchronous operation. In: *Proceedings of the 2002 IEEE Canadian conference on electrical & computer engineering*; 2002.
- [11] Arrouf M, Ghabrou S. Modelling and simulation of a pumping system fed by photovoltaic generator within the Matlab/Simulink programming environment. *Desalination* 2007;209.



**Mohammed Nabil** was born in Kafrelsheikh, Egypt in 1986. He received his B.Sc. degree in electrical engineering from Kafrelsheikh University, Egypt in 2008. He was appointed as a demonstrator at the Department of Electrical Engineering, Faculty of Engineering, Kafrelsheikh University in 2008. He is currently working towards the M.Sc. degree in Electrical Power and Machines Engineering at Faculty of Engineering, Tanta University, Egypt. His research interests are in

Electrical Machines, Electrical Drives, Power Electronics and renewable energy.



**Dr. Said M. Allam** was born in Basyun, Egypt in 1977. He received the B. Sc., M.Sc. and Ph.D degrees in Electrical Power and Machines Engineering from Tanta University, Egypt in 2000, 2004 and 2009, respectively. He is currently an assistant professor at the Department of Electrical Power and Machines Engineering, Faculty of Engineering, Tanta University. His research interests are in Electrical Machines, Electrical Drives, Power Electronics and renewable energy.



**Prof. Essam Eddin M. Rashad** was born in Shebin El-Kom, Egypt in 1960. He has graduated from Faculty of Engineering, Menoufiya University, Egypt on 1983. Then he obtained his MSc and PhD degrees in Electrical Engineering from Alexandria University, Egypt on 1987 and 1992 respectively. He has worked as an offshore maintenance engineer in Belayim Petroleum Company from 1985 to 1990. In 1992 he has joined Faculty of Engineering, Tanta University, Egypt, where

he is currently a Professor and Vice Dean for Education and Student affairs. His research interests include electrical machine analysis, electrical drives, power electronics and renewable energy. Prof. Rashad is an IEEE senior member since 2002.